HIGH-RESOLUTION IMAGE RECONSTRUCTION CONSIDERING INACCURATE MOTION INFORMATION

Min Kyu Park and Moon Gi Kang

Yonsei University
School of Electrical and Electronic Eng. Shinchon-dong,
Seodaemun-gu, Seoul, Korea

ABSTRACT

In this paper, we propose a high-resolution image reconstruction algorithm to reduce the distortion in the reconstructed high-resolution image due to the inaccuracy of motion estimation. For this purpose, we analyze the noise caused by the inaccurate motion information. Based on this analysis, we propose a new regularization functional. The proposed algorithm requires no prior information about the original image or the inaccurate motion information. Experimental results indicate that the proposed algorithm outperforms conventional approaches with respect to both objective and subjective criteria.

1. INTRODUCTION

Recently, a high-resolution image reconstruction handling inaccurate motion information has been researched [1]-[4]. In [1], the methods to reduce effects of inaccurate motion information were proposed. These methods are useful for improving the solution accuracy when errors exist not only in the recording process but also in the measurement matrix. Rafael $et\ al.$ proposed a method based on Bayesian approach [2]. However, the error caused by the inaccurate motion information only exists in the boundary of blur support since only uniform blur is considered. In [4], regularization functionals based on set theory were proposed. However, it depends on the initial condition.

In this paper, the perturbation caused by the motion estimation error is modeled as noise. To apply the noise model to regularization, we first analyze the noise caused by the motion estimation error. Since the noise caused by the motion estimation error in each channel is different, the regularization parameter is determined adaptively for each channel. The proposed regularization functional is determined automatically without any prior knowledge.

This research was supported by the MIC (Ministry of Information and Communication), Korea, under the ITRC (Information Technology Research Center) support program supervised by the IITA (Institute of Information Technology Assessment) (IITA-2005-(C1090-0502-0028))

The rest of the paper is organized as follows. In Section 2, the observation model based on the image acquisition system is briefly presented. In Section 3, the noise caused by the motion estimation error is analyzed. In Section 4, the regularization functional is chosen based on the analysis of the noise caused by the motion estimation error. With the regularization functional, a high-resolution image reconstruction is performed iteratively by gradient descent method. Experimental results are provided in Section 5. These include results obtained from simulated sequences and images acquired by a real system. Finally, some conclusions are given in Section 6.

2. PROBLEM FORMULATION

Consider the desired high-resolution image of size $N(=L_1N_1 \times L_2N_2)$ is written in lexicographical notation as the vector $\mathbf{x} = [x_1, \cdots, x_N]^T$. Here, parameters L_1 and L_2 are the downsampling factors for the horizontal and the vertical directions, respectively. Thus, each observed low-resolution image has size of $M(=N_1 \times N_2)$. Let the number of observed low-resolution images be p. The k-th low-resolution image can be denoted in lexicographic notation as $\mathbf{y}_\mathrm{k} = [\mathrm{y}_{\mathrm{k},1}, \cdots, y_{k,M}]^T$, for $k = 1, \cdots, p$. The observed low-resolution images which are degraded by motion, blur, downsampling, and noise are acquired from the high-resolution image $\mathbf{x}$. Then, the observation model can be written as

$$\mathbf{y_k} = \mathbf{D}\mathbf{B}_\mathrm{k}\mathbf{M}_\mathrm{k}(\mathbf{s}_\mathrm{k})\mathbf{x} + \mathbf{n}_\mathrm{k}, \quad for\ \ k = 1, 2, \cdots, p, \tag{1}$$

where the matrixes $\mathbf{D}$, $\mathbf{B}_\mathrm{k}$, and $\mathbf{M}_\mathrm{k}(\mathbf{s}_\mathrm{k})$ which represent downsampling, blur, and motion. The vector $\mathbf{s}_\mathrm{k}$ denotes the motion parameters of the k-th observation with respect to the desired high-resolution grid and $\mathbf{n}_\mathrm{k}$ is the additive zero mean Gaussian noise.

3. ANALYSIS OF NOISE CAUSED BY MOTION ESTIMATION ERROR

For simplifying expression, we consider 1-D signal instead of 2-D image to show the relationship between noise and inaccurate motion information. Let a continuous 1-D signal defined in $[0, T]$ and its shifted version be $s(t)$ and $s(t-\tau)$, respectively. Here, t and τ represent the time and the shift estimation error (motion estimation error in 2-D) via a original signal, respectively. In other words, $s(t)$ and $s(t-\tau)$ are an original signal and a signal with the shift estimation error. Thus, $n(t,\tau) = s(t) - s(t-\tau)$ becomes the noise caused by the shift estimation error. The mean of the noise $n(t,\tau)$ is defined as

$$\overline{n(t,\tau)} = \frac{1}{T}\int_0^T \big(s(t) - s(t-\tau)\big)\mathrm{dt}. \tag{2}$$

In order to get the solution of Eq.(2), we use the Taylor series expansion approximately

$$s(t-\tau) \approx s(t) + (-\tau)s'(t). \tag{3}$$

From Eq. (3), Equation (2) can be rewritten as

$$\begin{aligned}\overline{n(t,\tau)} &= \frac{1}{T}\int_0^T \tau s'(t)\mathrm{dt} \\ &= \tau\overline{s'(t)},\end{aligned} \tag{4}$$

where $\overline{s'(t)}$ is the mean value of the first differentiation of $s(t)$. The variance of $n(t,\tau)$ is defined as

$$\begin{aligned} var\big(n(t,\tau)\big) &= \frac{1}{T}\int_0^T \big(s(t) - s(t-\tau) - \overline{n(t,\tau)}\big)^2\mathrm{dt} \\ &= \frac{1}{T}\int_0^T \big(\tau s'(t) - \tau\overline{s'(t)}\big)^2\mathrm{dt} \\ &= \tau^2 var\big(s'(t)\big). \end{aligned} \tag{5}$$

We assume that the signal $s(t)$ has various increase or decrease patterns. According to this assumption, the mean of the first differentiation $s'(t)$ is nearly to zero. Thus, Equation (4) and Equation (5) can be rewritten as

$$\overline{n(t,\tau)} = 0, \tag{6}$$

and

$$var\big(n(t,\tau)\big) = \tau^2\overline{\big(s'(t)\big)^2}, \tag{7}$$

where $\overline{\big(s'(t)\big)^2}$ is the mean of square of the first differentiation.

4. HIGH-RESOLUTION IMAGE RECONSTRUCTION

The high-resolution image reconstruction is an ill-posed problem because of an insufficient number of low-resolution images, ill-conditioned blur operators, and inaccurate motion information. Constrained least squares (CLS) approach is the simplest method to solve this problem. A minimization functional of CLS in multichannel is defined as

$$F(\alpha, \mathbf{x}) = \sum_{\mathrm{k}=1}^{\mathrm{p}} \alpha\|\mathbf{y_k} - \mathbf{W_k x}\|^2 + \|\mathbf{Cx}\|^2, \tag{8}$$

where α denotes the regularization parameter and $\mathbf{C}$ is a high-pass operator. The choice of the regularization parameter is important since it controls the balance between fidelity to the data and smoothness of the solution. Each channel should be applied to different regularization parameters considering additive noise and the motion estimation error in each channel. Thus, Equation (8) can be changed into

$$F(\alpha_k(\mathbf{x}), \mathbf{x}) = \sum_{\mathrm{k}=1}^{\mathrm{p}} \alpha_{\mathrm{k}}(\mathbf{x})\|\mathbf{y_k} - \mathbf{W_k x}\|^2 + \gamma\|\mathbf{Cx}\|^2, \tag{9}$$

where $\alpha_k(\mathbf{x})$ and γ are the regularization functional considering the motion estimation error in each channel and the normalized parameter, respectively.

4.1. Choice of Multichannel Regularization Functional

In set theoretical approaches, the regularization functional $\alpha_k(\mathbf{x})$ in each channel is proportional to $\|\mathbf{Cx}\|^2$ and is inversely proportional to $\|\mathbf{y}_{\mathrm{k}} - \mathbf{W}_{\mathrm{k}}\mathbf{x}\|^2$. That is, the regularization functional $\alpha_k(\mathbf{x})$ in each channel is of the form

$$\alpha_k(\mathbf{x}) = \frac{\|\mathbf{Cx}\|^2}{\|\mathbf{y}_{\mathrm{k}} - \mathbf{W}_{\mathrm{k}}\mathbf{x}\|^2 + \delta_{\mathrm{k}}}, \tag{10}$$

where δ_k is a parameter preventing the denominator from becoming zero. Since the residual term $\|\mathbf{y}_{\mathrm{k}} - \mathbf{W}_{\mathrm{k}}\mathbf{x}\|^2$ decreases rapidly in the iteration procedure, the residual term $\|\mathbf{y}_{\mathrm{k}} - \mathbf{W}_{\mathrm{k}}\mathbf{x}\|^2$ becomes close to zero. This makes it difficult that the minimization functional has an optimal solution in which every channel is considered. For example, when one channel has no motion estimation error, the regularization functional in the channel is close to infinite and the other channels are not considered in the regularization. In order to solve this problem, Lee and Kang proposed two regularization functionals to prevent them from decreasing suddenly and to consider the influence of the cross-channel [4]. However, this depends on the initial condition. For example, if the initial condition of $\mathbf{x}$ is an image with constant values, then $\|\mathbf{Cx}\|^2$ is zero. This makes it difficult to have an optimum solution by minimizing the minimization functional in the iteration.

We propose a regularization functional which considers the noise caused by the motion estimation error. The regularization functional should be determined by considering the motion estimation error in the channel and the relationship between it and the other channels. Let the motion estimation error in k-th channel be e_k. The regularization functional should be inversely proportional to e_k, *i.e.*

$$\alpha_k(\mathbf{x}) \propto \frac{1}{e_k^2}. \tag{11}$$

Among various inversely proportional candidate functions, we choose the inversely proportional function as

$$\alpha_k(\mathbf{x}) \propto \exp(-\mathrm{e}_{\mathrm{k}}^2). \tag{12}$$

Motion	Case1	Case2	Case3	Case4
$(\delta_{h,1}, \delta_{v,1})$	(0.0,0.0)	(0.0,0.0)	(0.2,0.2)	(0.0,0.0)
$(\delta_{h,2}, \delta_{v,2})$	(0.1,0.2)	(0.1,0.4)	(0.0,0.2)	(-0.1,0.2)
$(\delta_{h,3}, \delta_{v,3})$	(0.4,0.1)	(0.4,0.2)	(0.5,0.0)	(0.3,-0.1)
$(\delta_{h,4}, \delta_{v,4})$	(0.5,0.5)	(0.3,0.3)	(0.4,0.4)	(0.4,0.3)

Table 1. The inaccurate motion compared with the accurate sub-pixel motion information $\{(\delta_{h,k}, \delta_{v,k}) | (0.0, 0.0), (0.0, 0.5), (0.5, 0.0), (0.5, 0.5)\}$, for $k = 1, 2, 3, 4$.

As it has been mentioned in Sec.3, the variance of the noise caused by e_k is proportional to the multiplication of e_k^2 and the high-frequency energy. In other words, e_k^2 is proportional to the variance of the noise caused by e_k and is inversely proportional to the high-frequency energy. Therefore, Equation (12) can be rewritten as

$$\alpha_k(\mathbf{x}) \propto \exp(-\frac{\|\mathbf{y}_\mathrm{k} - \mathbf{W}_\mathrm{k}\mathbf{x}\|^2}{\|\mathbf{C}\mathbf{x}\|^2}). \tag{13}$$

Since $\|\mathbf{C}\mathbf{x}\|^2$ is the same value in every channel, $\|\mathbf{C}\mathbf{x}\|^2$ can be changed into a parameter $\mathrm{P_G}$. Therefore, we choose the regularization functional $\alpha_k(\mathbf{x})$ as

$$\alpha_k(\mathbf{x}) = \exp(-\frac{\|\mathbf{y}_\mathrm{k} - \mathbf{W}_\mathrm{k}\mathbf{x}\|^2}{\mathrm{P_G}}). \tag{14}$$

4.2. Gradient Descent Optimization

We consider a gradient descent method for minimizing the minimization functional in Eq.(9) and estimate a high-resolution image. The update procedure for an estimate can be written as

$$\hat{\mathbf{x}}_\mathrm{r}^{\mathrm{n}+1} = \hat{\mathbf{x}}_\mathrm{r}^\mathrm{n} - \beta^\mathrm{n} \nabla_\mathbf{x} \mathrm{F}(\alpha_\mathrm{k}(\hat{\mathbf{x}}^\mathrm{n}), \hat{\mathbf{x}}^n), \tag{15}$$

for $n = 0, 1, 2, \cdots$ and $r = 1, \cdots, N$. These partial derivatives are given by differentiating Eq.(9)

$$\nabla_\mathbf{x} F(\alpha_k(\mathbf{x}), \mathbf{x}) = \sum_{\mathbf{k=1}}^{\mathbf{p}} \Big\{ \mathbf{2}\alpha_\mathbf{k}(\mathbf{x}) \mathbf{W}_\mathrm{k}^\mathrm{T} (\mathbf{W}_\mathrm{k}\mathbf{x} - \mathbf{y}_\mathrm{k}) + \nabla_\mathbf{x} \alpha_k(\mathbf{x}) \|\mathbf{y}_\mathrm{k} \mathbf{W}_\mathrm{k}\mathbf{x}\|^2 \Big\} + 2\gamma \mathbf{C^T C x}, \tag{16}$$

where $\alpha_k(\mathbf{x})$ is differentiated Eq.(14) is used as

$$\nabla_\mathbf{x} \alpha_k(\mathbf{x}) = 2\alpha_\mathrm{k}(\mathbf{x}) \mathbf{W}_\mathrm{k}^\mathrm{T} (\mathbf{W}_\mathrm{k}\mathbf{x} - \mathbf{y}_\mathrm{k}) \Big(\frac{1}{\mathrm{P_G}}\Big). \tag{17}$$

Equation (16) can be rewritten as

$$\nabla_\mathbf{x} F(\alpha_k(\mathbf{x}), \mathbf{x}) = \sum_{\mathrm{k=1}}^{\mathrm{p}} \alpha'_k(\mathbf{x}) {\mathbf{W}_\mathrm{k}}^\mathrm{T} (\mathbf{W}_\mathrm{k}\mathbf{x} - \mathbf{y}_\mathrm{k}) + 2\gamma \mathbf{C^T C x}, \tag{18}$$

PSNR(dB)	Case1	Case2	Case3	Case4
Bi-cubic	23.721	23.721	23.721	23.721
CM1	27.688	27.140	27.068	26.364
CM2	28.847	28.214	28.096	27.885
PM	30.476	29.888	28.944	28.179

Table 2. The PSNR of the conventional reconstruction algorithms and the proposed algorithm when the sub-pixel motion is as in Table 1.

where

$$\alpha'_k(\mathbf{x}) = 2\alpha_\mathrm{k}(\mathbf{x}) \Big(1 - \frac{\|\mathbf{y}_\mathrm{k} - \mathbf{W}_\mathrm{k}\mathbf{x}\|^2}{\mathrm{P_G}}\Big). \tag{19}$$

Since both $\alpha_k(\mathbf{x})$ and $\Big(1 - \frac{\|\mathbf{y}_\mathrm{k} - \mathbf{W}_\mathrm{k} x\|^2}{\mathrm{P_G}}\Big)$ consider motion estimation error, $\alpha'_k(\mathbf{x})$ that is a multiplication of $\alpha_k(\mathbf{x})$ and $\Big(1 - \frac{\|\mathbf{y}_\mathrm{k} - \mathbf{W}_\mathrm{k} x\|^2}{\mathrm{P_G}}\Big)$ is more sensitive to motion estimation error than $\alpha_k(\mathbf{x})$. $\alpha'_k(\mathbf{x})$ control the update rate in each channel. That is, a channel with less motion estimation error is more updated. On the other hand, a channel with much motion estimation error is less updated.

5. EXPERIMENTAL RESULTS

We set γ to be 0.2. $\mathrm{P_G}$ is chosen to be $\big(3 \times \max(\|\mathbf{y}_1 - \mathbf{W}_1\mathbf{x}\ \|^2, \cdots, \|\mathbf{y}_\mathrm{p} - \mathbf{W}_\mathrm{p}\mathbf{x}\|^2)\big)$. To compare with the proposed algorithm, two reconstruction algorithms were used. One is a CLS-based high-resolution reconstruction algorithm described in [5]. We refer to this method as CM1. The other referred to as CM2 is a reconstruction algorithm in [4] with the irrational regularization functional. Four low-resolution images are synthetically generated from a high-resolution shop image which is translated with one of the sub-pixel shifts $\{(0, 0), (0, 0.5), (0.5, 0), (0.5, 0.5)\}$, blurred, decimated by a factor of two in both the horizontal and vertical directions. Although the motion information of the simulated low-resolution images is known exactly, we assume that the motion estimation is inaccurate, as in the four cases shown in Table 1.

The partially magnified results of high-resolution image reconstruction algorithms are shown in Fig.1. These results are obtained by using Case 2 in Table 1. The bi-cubic interpolated image is the poorest among the results since one low-resolution image is only considered in the reconstructing process. Compared to this method, the results of CM1 is improved. However, since CM1 does not consider the inaccurate motion information in each channel, the result of CM1 has visual artifacts like white or black dot near edge. These visual artifacts can be reduced by increasing the regularization parameter. However, this make the result to be over-smooth or to lose important high-frequency components. To obtain better solution, many trial and error tests or additional information for the motion is needed. On the other hand, the results of CM2 and PM are are satisfactory in that the high

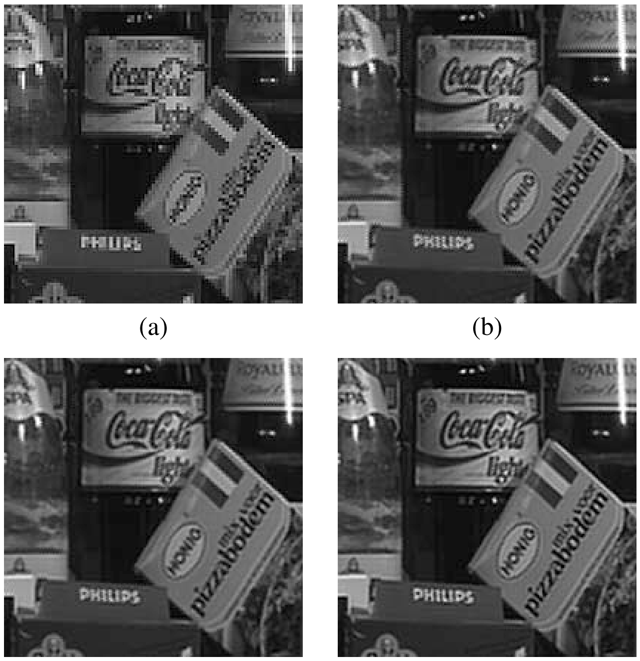

(a) (b)

(c) (d)

Fig. 1. Partially-magnified images of results from shop image : Reconstructed image by (a) Bi-cubic interpolation, (b) CM1, (c) CM2, and (d) PM.

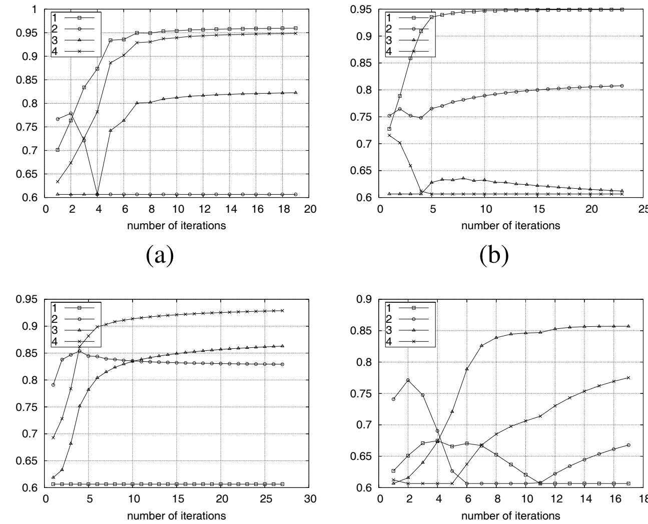

(a) (b)

(c) (d)

Fig. 2. The proposed regularization functional $\alpha_k(\mathbf{x})$, $k = 1, 2, 3, 4$, (a) Case1, (b) Case2, (c) Case3, and (d) Case4.

frequency of the reconstructed image is conserved while suppressing the noise caused by the inaccurate motion information. The PSNR of the reconstructed high-resolution image for the four cases in Table 1 are presented in Table 2. This table shows the proposed algorithm outperform the conventional methods. To validate the proposed algorithm, The regularization functional versus the number of iteration for the four cases in Table 1 is shown in Fig.2. These figures show the values of the regularization functionals $\alpha_k(\mathbf{x})$ are determined automatically according to the accuracy of the motion information in each channel. This helps the proposed algorithm to distinguish the channel with the inaccurate motion information from the channel with the accurate motion information.

6. CONCLUSION

In this paper, we proposed a high-resolution image reconstruction algorithm to reduce the distortion caused by the inaccurate motion information. To facilitate these, we analyzed the noise caused by the inaccurate motion information. Based on this analysis, we proposed a new regularization functional. Since the proposed regularization functional is inversely proportional to the noise, the distortion caused by the inaccurate motion information is reduced clearly.

7. REFERENCES

[1] M. K. Ng, and N. K. Bose, "Analysis of displacement errors in high-resolution image reconstruction with multisensors," *Circuits and Systems I: Fundamental Theory and Applications, IEEE Transactions on,* vol.49, Issue.6, pp.806-813, Jun., 2002.

[2] M. Rafael, V. Miguel, A. Javier, and A. K. Katsageelos, "Parameter estimation in bayesian high-resolution image reconstruction with multisensos", *IEEE Transactions on Image Processing,* vol.12, no.12, pp.1655-1667, Dec. 2003.

[3] M. Park, E. Lee, J. Park, M. G. Kang, and J. Kim, " DCT-Based High-Resolution Image Reconstruction Considering the Inaccurate Sub-Pixel Motion Information", *SPIE Optical Engineering*, vol.41, no.2, pp.370-380, Feb. 2002.

[4] E. Lee, and M. Kang, "Regularized adaptive high-resolution image reconstruction considering inaccurate subpixel registration," *IEEE Transactions on Image Processing,* vol.12, no.7, pp.826 837, July 2003

[5] R. C. Hardie, K. J. Barnard, J. G. Bognar, E. E. Armstrong, and E. A. Watson, "High-resolution image reconstruction from a sequence of rotated and translated frames and its application to an infrared imaging system," *SPIE Optical Engineering,* vol.37, no.1, pp.247-260, Jan., 1998.